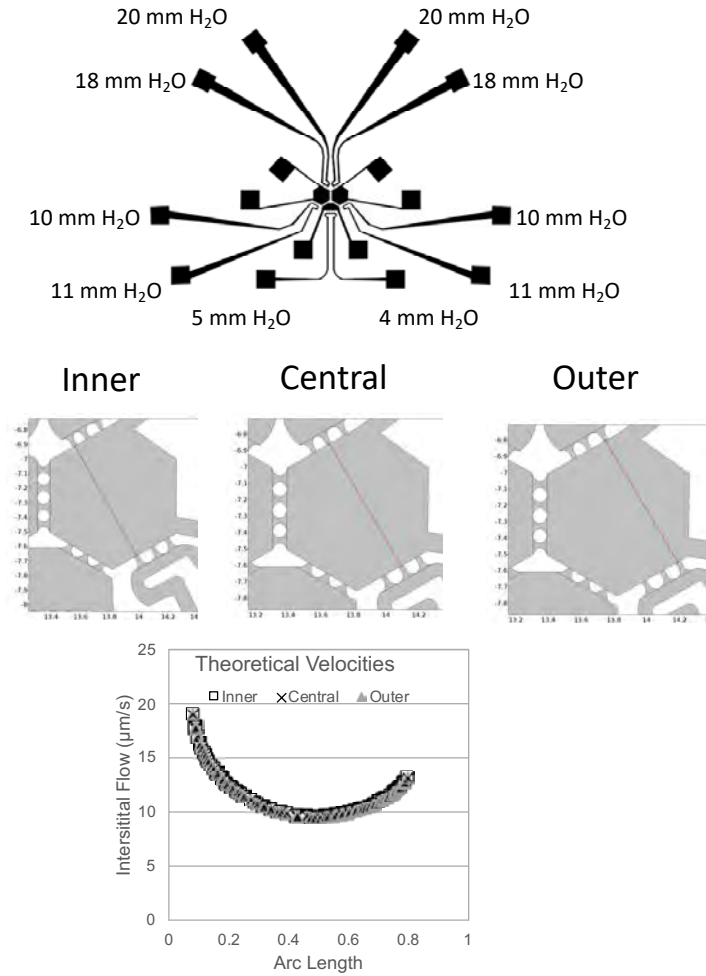
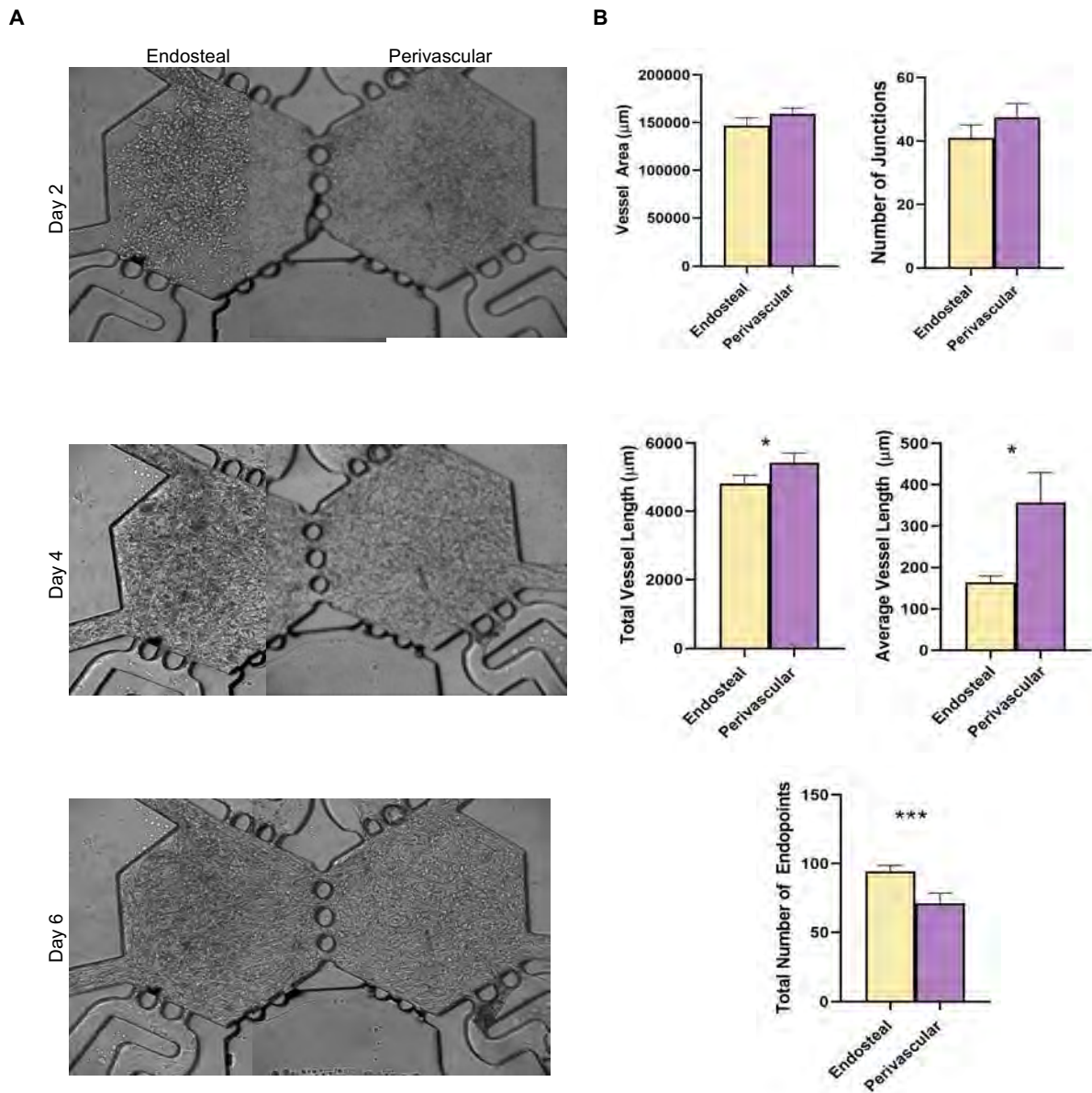


1 Supplementary Materials



Supplemental Figure 1

2
3 **Figure S1. Theoretical modeling of interstitial flow in the device.** Schematic of the device, including the pressure
4 used in each fluidic line to produce the desired interstitial flow. Three arbitrary lines drawn through the ports of the
5 device. Theoretical modeling in COMSOL demonstrated similar interstitial velocity through all three ports when the
6 device is filled with fibrin gel.



Supplemental Figure 2

7

8 **Figure S2. Characterization of vessel networks in the endosteal and perivascular niches of the BMoac.** (A)

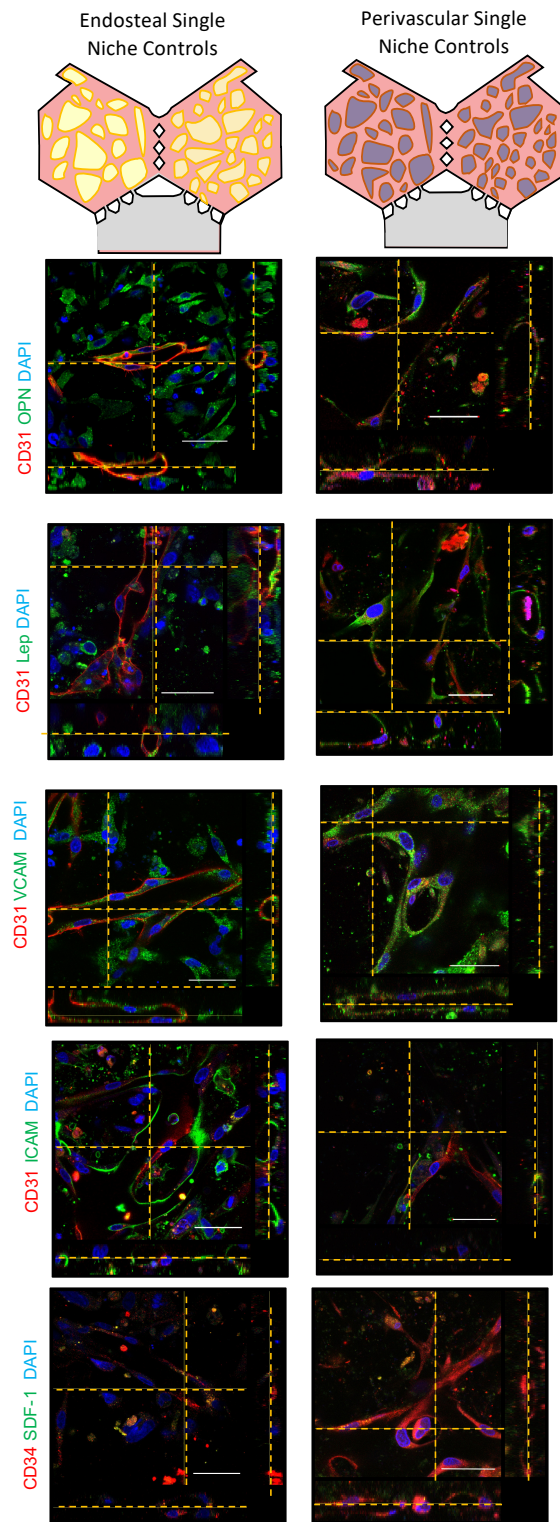
9 Microvascular networks self-assembled from a cell suspension (Day 2) into vascular fragments (Day 4) and an

10 interconnected network (Day 6). (B) Vascular networks stained for either CD34 or CD31 in Fig. 2 and Fig. 3 were

11 characterized using Angiotool. Mean with SEM shown for total vessel area (top), total vessel length (middle), and

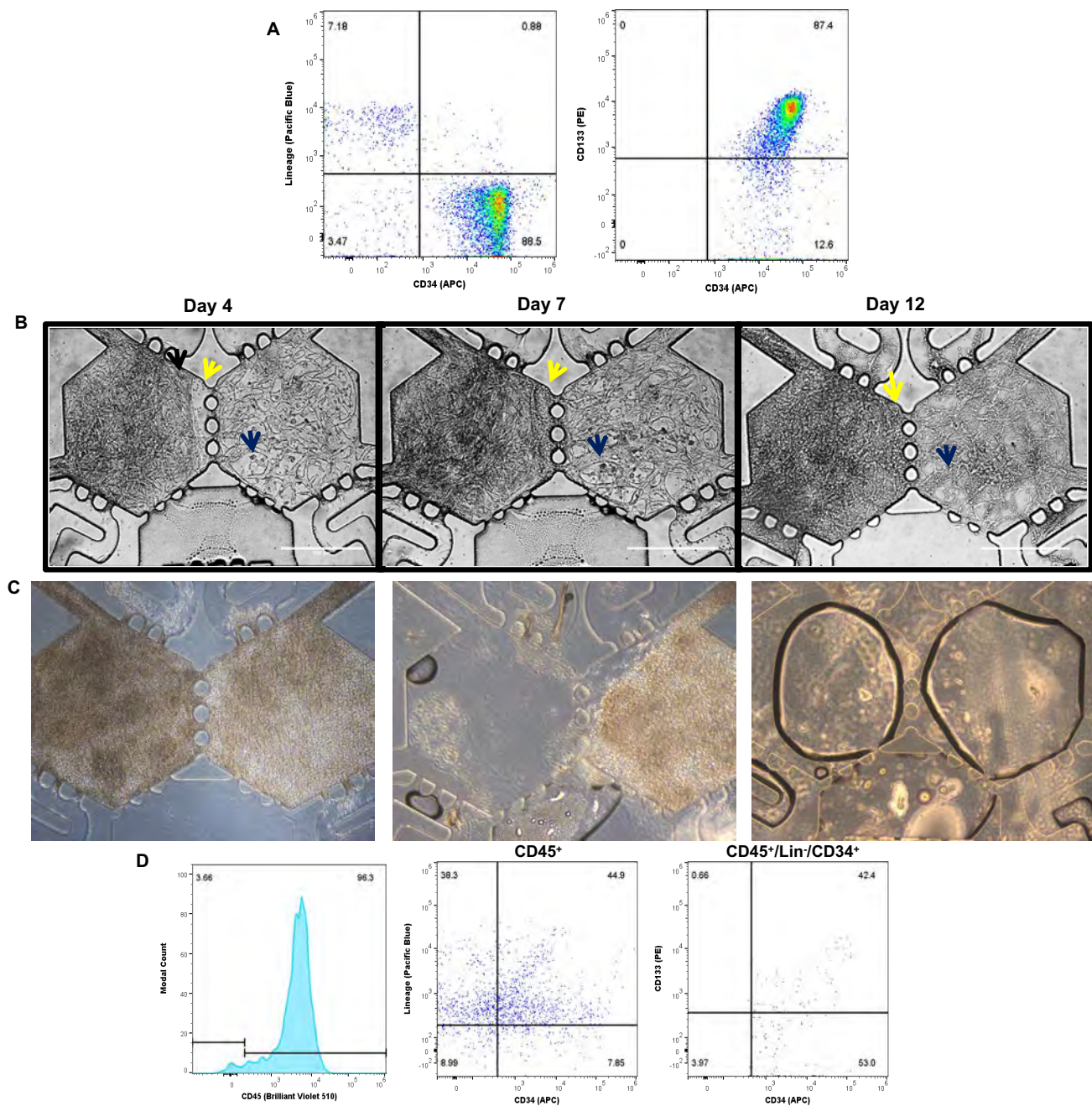
12 total number of endpoints (bottom); n=10. *p<0.05, **p<0.01, paired t-test.

13



Supplemental Figure 3

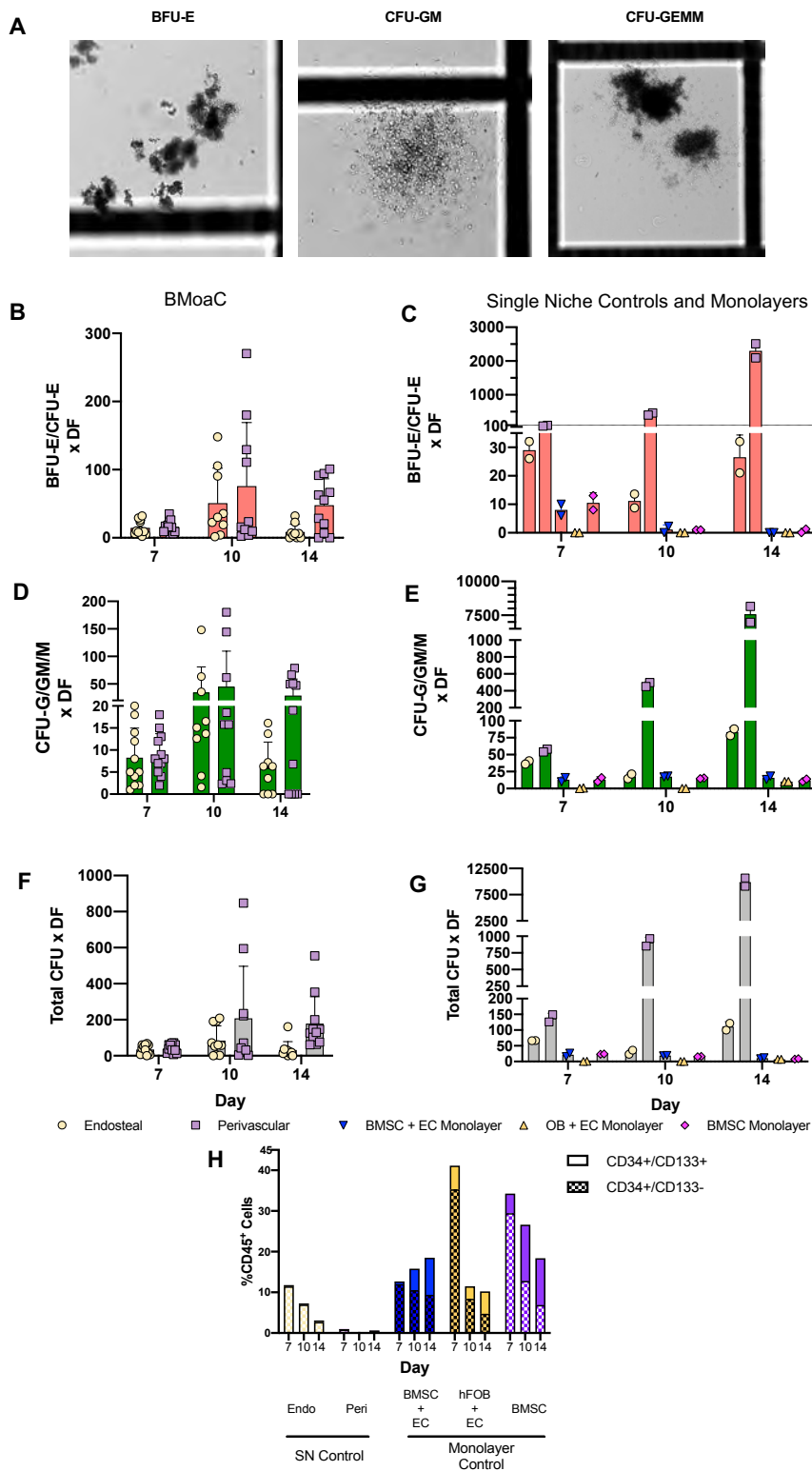
14
 15 **Figure S3. Single niche controls expressed markers associated with *in vivo* bone marrow.** Endothelial cells
 16 (CD34 or CD31, red) and osteopontin, leptin, VCAM-1, ICAM-1, and SDF-1 (all green). Nuclei were counterstained
 17 with DAPI (blue). Scale bar: 50 μ m. Expression of SDF-1/CXCL-12 was muted in the single niche perivascular
 18 control compared to the BMoAC.



Supplemental Figure 4

19

20 **Figure S4. Characterization of HSPC prior to loading in, during culture in, and following recovery from the**
 21 **BMoAC. (A)** Representative flow cytometry plot of Lin⁻/CD34⁺ and CD133⁺/CD34⁺ cells isolated from cord blood.
 22 These cells were later cultured in the BMoAC as HSPC. **(B)** CD34⁺ cells proliferated in the device during the 14 day
 23 culture period. Yellow and dark blue arrows highlight CD34-derived cells in the endosteal and perivascular niches,
 24 respectively. Scale bar: 500 μ m. **(C)** Representative images of a device digested with 10 U/mL nattokinase. Cells
 25 from each niche were isolated separately for downstream analysis. **(D)** Representative flow cytometry plot of cells
 26 collected from the perivascular niche following digestion of the device on Day 10.



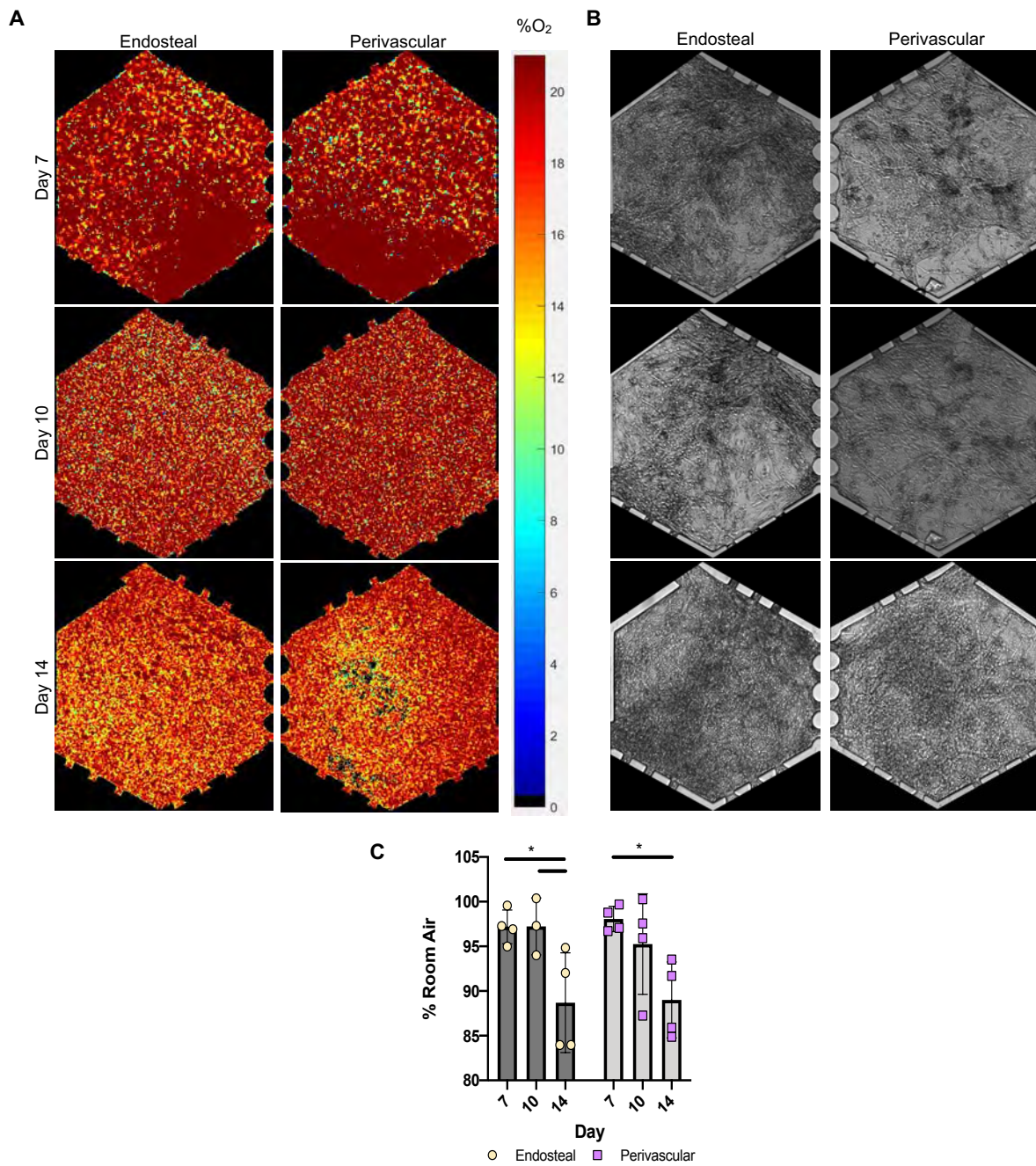
Supplemental Figure 5

27

28 **Figure S5. Functional characterization and quantification of HSPC isolated from BMoAC, SN controls, and**
 29 **monolayer controls. (A)** Representative images of CFU colonies generated by cells collected from BMoAC devices
 30 following 14 days of culture. Colonies were quantified according to their morphology. **(B, D, F)** BMoAC, **(C, E, G)**
 31 SN, and monolayer controls showed different CFU potential for **(B, C)** erythroid and **(D, E)** myeloid lineages. There

32 were no significant differences between the endosteal and the perivascular niches of the BMoac; both niches
33 supported erythroid and myeloid CFU and had a similar number of total colonies, biological replicates with n=10-11.
34 SN controls supported erythroid and myeloid CFU. Monolayer controls, including CD34⁺ cells cultured on BMSC,
35 had a limited ability to support cells with erythroid CFU potential past day 7 or to support cells with myeloid CFU
36 potential. **(F, G)** The total number of CFU was much higher in the SN than the monolayer controls. **(H)** SN and
37 monolayer controls differed in their ability to maintain a stem/progenitor cells (CD34⁺/CD133⁺ and CD34⁺/CD133⁻)
38 over time.

39



Supplemental Figure 6

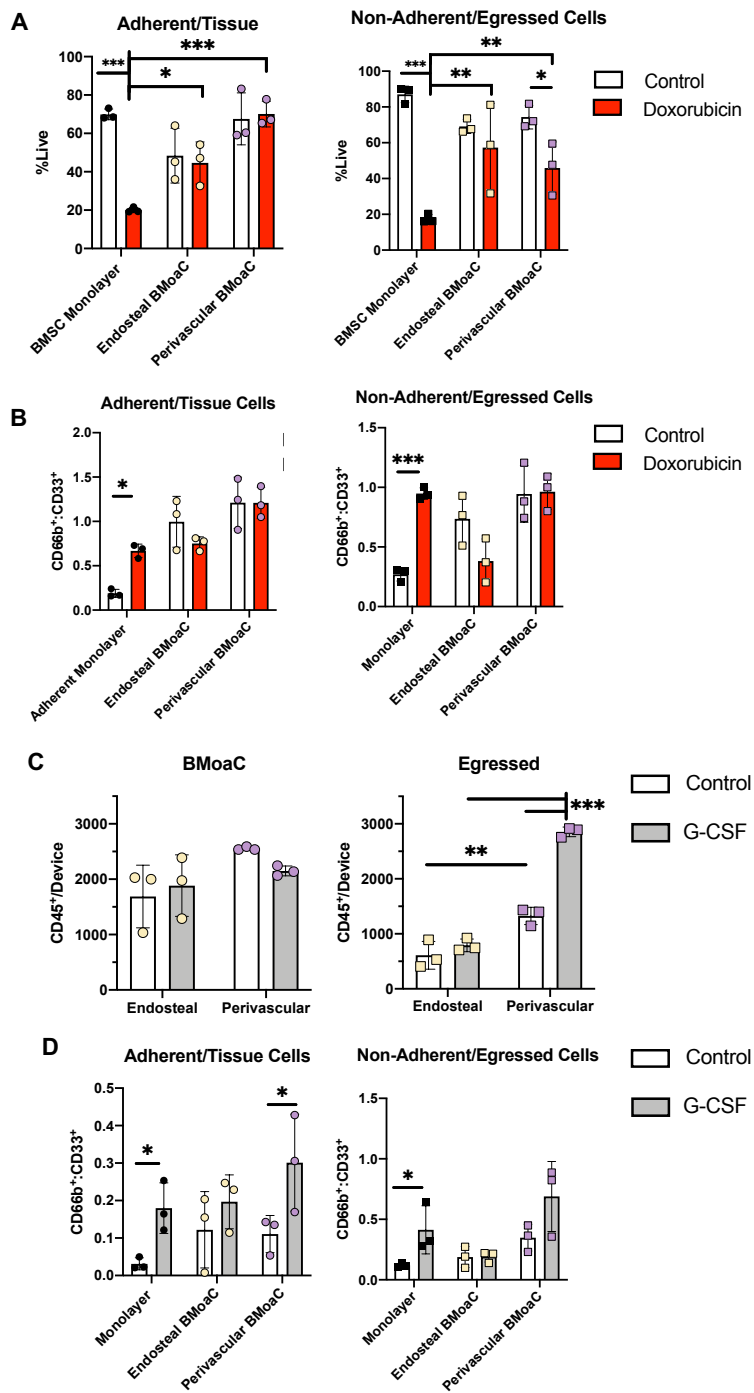
40

41 **Figure 6. O₂ tension in the endosteal and perivascular niches of the BMoaC decreased over time. (A)** Maps of

42 O₂ tension in the endosteal (left) and perivascular (right) chambers of a BMoaC device on days 7, 10, and 14.

43 Measurements were collected using phosphorescence lifetime imaging microscopy (PhLIM) and the oxygen sensitive

44 dye Oxyphor G4. **(B)** Brightfield images of the tissue chambers from panel A.



Supplemental Figure 7

48

49

50 **Figure S7. Treatment with doxorubicin or G-CSF altered cell populations in the BMoaC and monolayer**

51 **controls. (A)** Exposure to 0.5 M Doxorubicin for 48 hours significantly reduced the viability of both non-adherent
52 and adherent cells in the monolayer control (**p<0.0001, 2-way ANOVA with Sidak's post hoc comparison). In the

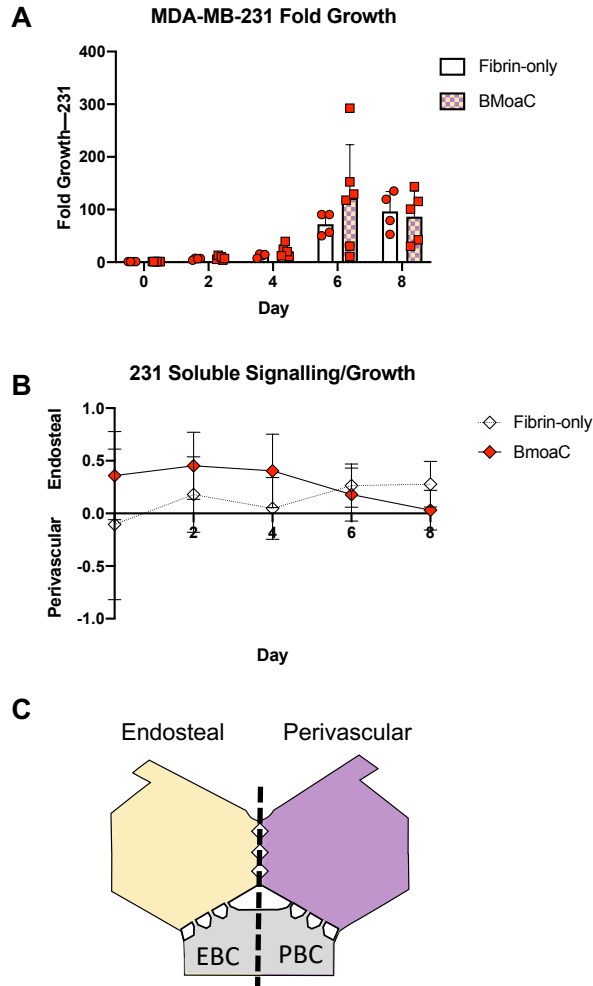
53 BMoaC, cell viability was reduced only in egressed cells from the perivascular niche. **(B)** Doxorubicin significantly

54 increased the ratio of CD66b+:CD33+ cells for both adherent and non-adherent cells in the monolayer control

55 (*p<0.05, *** p<0.0001, respectively 2-way ANOVA with Sidak's post hoc comparison), but did not affect the ratio

56 in the BMoaC. **(C)** Exposure to 30 ng/mL of G-CSF did not change the number of tissue resident cells in either niche
57 of the BMoaC. In contrast, egressed cells from the perivascular niche increased significantly compared to control
58 niches and treated endosteal niches (from the same devices; ** $p < 0.01$, *** $p < 0.0001$, 2-way ANOVA with Tukey's
59 post hoc comparison test). **(D)** G-CSF significantly increased the ratio of CD66b⁺:CD33⁺ cells for both adherent and
60 non-adherent cells in the monolayer control. In the BMoaC, this ratio was significantly increased only in tissue
61 resident cells from the perivascular niche (* $p < 0.05$, 2-way ANOVA with Sidak's post hoc comparison).

62
63
64



$$\text{Soluble Signaling/Growth} = \frac{EBC_{TX} - PBC_{TX}}{EBC_{TX} + PBC_{TX}}$$

Supplemental Figure 8

67

68 **Figure S8. Characterization of MDA-MB-231 growth kinetics and response to soluble signaling in the BMoaC.**69 **(A)** Cancer cell growth in the bottom chamber of fibrin-only and BMoaC devices was quantified over 9 days via a70 change in fluorescent area. **(B)** Growth on either side of the bottom chamber and overall growth were compared to

71 assess the bias, if any, introduced by soluble signaling from the endosteal or perivascular niches. Positive and

72 negative values indicated biased growth towards the endosteal and perivascular sides, respectively. There was no

73 statistical difference from 0 over time. **(C)** A cartoon representation of the BMoaC device depicting the method used

74 to analyze the effect of soluble signaling on growth. EBC: Endosteal half of the bottom chamber, PBC: Perivascular

75 half of the bottom chamber, *TX*: Time X.

76

77

78 **Table S1. Immunofluorescent antibodies.** Antibodies were used at 1:100 unless otherwise noted.

79

<i>Antigen</i>	<i>Fluorophore/host</i>	<i>Vendor</i>	<i>Cat #</i>
CD34	APC	BioLegend	343510
Laminin	Alexa Fluor 488	Novus Biologicals	NB300-144AF488
CD54	Alexa Fluor 488	BioLegend	322713
CD62E	APC	BD Biosciences	551144
CXCL-12	PE	R&D Systems	IC350P
Nestin	Alexa Fluor 488	ThermoFisher	53-9843-80
CD90	FITC	BioLegend	328108
CD14	Brilliant Violet 421	BioLegend	325628
Lineage	Pacific Blue	BioLegend	348805
CD31 (JC/70A)	Mouse	ThermoFisher	MS-353-S
VCAM-1	Rabbit	Abcam	ab134047
Osteopontin*	Rabbit	Abcam	ab8448
Leptin	Rabbit	ThermoFisher	PA1-052
Goat anti-Rabbit IgG*	Alexa Fluor 488	Invitrogen	A-11008
Goat anti-Mouse IgG*	Alexa Fluor 555	Invitrogen	A-21422
SytoxOrange	N/A	ThermoFisher	S11368
DAPI	N/A	ThermoFisher	D1306

80 *Used at 1:1000

81

82 **Table S2. Flow cytometry antibodies.** Antibodies were used in a final volume of 100 μ L.

83

<i>Antigen</i>	<i>Fluorophore</i>	<i>Vendor</i>	<i>Cat #</i>	<i>Vol. per test</i>
CD14	Alexa Fluor 700	BioLegend	325614	5 μ L
CD15	APC/Cy7	BioLegend	323048	5 μ L
CD33	Brilliant Violet 510	BioLegend	366610	5 μ L
CD34	APC	BioLegend	343510	5 μ L
CD45	FITC	BioLegend	368508	5 μ L
CD133	PE	BioLegend	372804	5 μ L
Lineage	Pacific Blue	BioLegend	348805	20 μ L
Live/Dead	Fixable Yellow	ThermoFisher	L34959	1 μ L

84

85

86

87 **Movie S1. Microvascular networks in the BMoac were perfused with 70 kDa TRITC-dextran.**

88

89 **Movie S2. CD34⁺-derived cells migrated through the device, into the fluidic lines, and to the adjacent chamber.**

90 10-hour timelapse video of a BMoac on Day 6 of culture. Images were acquired every twenty minutes.

91

92 **Movie S3. Confocal Z-stack of the BMoac endosteal niche.** In the region shown in Fig. 3Ci, a blood vessel

93 surrounds a colony of CD34⁺ (red) and Lin⁺ (green) cells in the endosteal niche.

94

95 **Movie S4. Confocal Z-stack of the BMoac perivascular niche.** In the region shown in Fig. 3Cii, CD34⁺ (red) and

96 Lin⁺ (green) are seen coming in and out of focus. A blood vessel is located on the left side of the images.

97

98